Pressure-induced liquid-liquid transition in a family of ionic materials

Zaneta Wojnarowska (zaneta.wojnarowska@smcebi.edu.pl)
University of Silesia in Katowice https://orcid.org/0000-0002-7790-2999
Shinian Cheng
University of Silesia in Katowice https://orcid.org/0000-0002-5615-8646
Malgorzata Swadzba-Kwasny
The QUILL Research Centre https://orcid.org/0000-0003-4041-055X
Shannon McLaughlin
The QUILL Research Centre
Yoan Delavoux
The QUILL Research Centre
Marian Paluch
University of Silesia in Katowice

Article

Keywords: liquid–liquid transition (LLT), ionic materials, Clausius-Clapeyron equation

Posted Date: June 4th, 2021

DOI: https://doi.org/10.21203/rs.3.rs-557473/v1

Pressure-induced liquid-liquid transition in a family of ionic materials

Z. Wojnarowska[1*], S. Cheng[1], M. Swadzba-Kwasny[2], S. McLaughlin,[2] Y. Delavoux,[2] M. Paluch[1]

[1]*Institute of Physics, the University of Silesia in Katowice, Silesian Center for Education and Interdisciplinary Research, 75 Pułku Piechoty 1A, 41–500 Chorzów, Poland*
[2] *The QUILL Research Centre, School of Chemistry and Chemical Engineering, The Queen's University of Belfast, David Keir Building, Stranmillis Rd, BT9 5AG, Belfast, NI, UK*

**corresponding author zaneta.wojnarowska@smcebi.edu.pl*

Liquid−liquid transition (LLT) between two disordered phases of single-component material remains one of the most intriguing physical phenomena. Here, we report a first-order LLT in a series of ionic liquids containing trihexyl(tetradecyl)phosphonium cation $[P_{666,14}]^+$ and anions of different sizes and shapes, providing an insight into the structure-property relationships governing LTT. In addition to calorimetric proof of LLT, we report that ion dynamics exhibit anomalous behavior during the LLT, i.e., the conductivity relaxation times (τ_σ) are dramatically elongated, and their distribution becomes broader. This peculiar behavior is induced by both isobaric cooling and isothermal compression with the $\tau_\sigma(T_{LL},P_{LL})$ being constant for a given system. The latter observation proves that LLT, in analogy to liquid-glass transition, has an isochronal character. Finally, the magnitude of discontinuity in a specific volume at LLT was examined using the Clausius-Clapeyron equation.

When isotropic liquid is cooled below the melting point, it either solidifies into a crystal or enters into a metastable supercooled state, which then enters a non-equilibrium amorphous phase at the glass transition temperature, T_g.[1] The characteristic feature of the latter transformation is a continuous increase of density, accompanied by slowing down of molecular dynamics and enormous elongation of structural relaxation times: from the time scale of picoseconds at T_m up to hundreds of seconds in the vicinity of T_g.[2] If cooled rapidly enough, nearly all materials can be transformed into an amorphous form. Thus, the glass-forming ability can be considered as a universal property of condensed matter.

Over the years, such a well-established physical picture of liquid state has been upended by numerous examples on two distinct liquid phases exiting in single-component materials. The first-order liquid-liquid transition (LLT), separating fluids of different local structures, density and thermodynamic properties, has been reported for various systems, including atomic elements (sulfur, phosphorus[3], silicon[4,5], carbon[6]) and strongly interacting liquids[7], such as molten oxides[8,9], e.g. Al_2O_3-Y_2O_3.[10] Only four molecular liquids (water[11,12], triphenyl phosphate (TPP)[13,14,15], n-butanol, and D-mannitol) have been found with compelling evidence for LLT. Nevertheless, the LLT in these systems remains controversial, since it occurs in the supercooled state capable of cold crystallization.[16] The theoretical permits and experimental observations that a first-order LLT can take place without a noticeable density change make this phenomenon even more puzzling.[17] At the same time, nothing is known about the effect of molecular packing on LLT, except for a

few simple cases.[18,19] Consequently, it has not been clarified how universal the LLT is and what is the critical factor inducing such a transition. Since it has been difficult to identify other examples of LLT in a systematic fashion, the experimental verification of these problems poses a great challenge.

Aprotic ionic liquids (AILs) – a class of glass-formers composed solely of ions[20], gives a unique opportunity to investigate the universality of LLT. The most interesting feature of AILs is that their structural and transport properties can be finely tuned within a wide range by the combination of different positively and negatively charged ions.[21] Thereby, a vast structural diversity of ionic species and various types of competing intermolecular interactions (van der Waals, H-bonding and Coulomb forces), make AILs excellent materials to probe the mechanism underpinning LLT. The first prove of LLT in an aprotic ionic liquid has been reported very recently by Harris et al., and observed in an AIL with a tetraalkylphosphopnium cation.[22] At a specific temperature, trihexyl(tetradecyl)phosphonium borohydride, noted as $[P_{666,14}][BH_4]$, was found to undergo enhanced ordering of the alkyl chains in the nonpolar domains. Such a structural reorganization coincides well with the first-order thermodynamic transition, visible in calorimetric, XRD and IR spectroscopy data.

Motivated by this work, we embarked on a quest to identify not an isolated example, but a systematically studied family of compounds that would exhibit LTTs, thereby gaining, for the first time, an insight into the structure-property relationships governing the LTT formation. Furthermore, by monitoring the relaxation dynamics of selected AILs under high-pressure conditions, we addressed the long-standing questions regarding the effect of compression on liquid-liquid transition and density fluctuations at T_{LL}.

We designed six AILs based on the $[P_{666,14}]^+$ cation, combined with six different anions (chemical structures shown in Figure 1). The commonly used phosphonium cation imparted the AILs a relatively high thermal and electrochemical stability, as well as decent ionic conductivity and apolar/polar solvation ability.[23] Anions have been selected to reflect differences in size, geometry, conformational flexibility and coordinating ability (i.e. Lewis basicity). The linear thiocyanate, $[SCN]^-$, trigonal planar tricyanomethanide, $[TCM]^-$ and tetrahedral $[BF_4]^-$ are all rigid due to their small size. The larger anions include a bulky and rigid $[BOB]^-$, with distorted tetrahedral symmetry around the central boron atom, the $[TFSI]^-$ that is known to assume *cis* and *trans* conformations, and $[TAU]^-$, featuring a flexible alkyl chain allowing for multiple conformations. Lewis basicity of non-coordinating $[BF_4]^-$, very weekly-coordinating $[TFSI]^-$, a weakly basic $[TCM]^-$ and coordinating $[SCN]^-$ is listed in Table 1. The two anions that have not been measured are qualitatively known to lie on the opposite sides of the scale: $[BOB]^-$ is extremely weakly coordinating, and $[TAU]^-$ has an amine functionality, which by definition imparts it Lewis acidity.

Results and Discussion

Calorimetric studies of phase transitions. To firmly establish the LLT scenario, it is desirable to show its reversibility without crystallization. For this purpose, we firstly analyzed the conventional DSC thermograms obtained on cooling and subsequent heating of tested materials (Figure 1). Decreasing temperature with a standard rate of 10 K/min resulted in a step-like transition for $[P_{666,14}][BOB]$, a sharp exothermic peak at 226 K for $[P_{666,14}][BF_4]$, and broader

exothermic peaks at 200±10 K for the other four AILs. On heating, the thermal curve for $[P_{666,14}][BOB]$ featured a glass transition, symmetrical with respect to the cooling scan. Sharp endotherms, quite symmetrical with respect to the cooling cycles, were recorded for $[P_{666,14}][TAU]$, $[P_{666,14}][TFSI]$ and $[P_{666,14}][TCM]$. For $[P_{666,14}][SCN]$, an endothermic peak was recorded ca. 200 K, followed by cold crystallisation and melting upon further heating. Finally, endotherm for $[P_{666,14}][BF_4]$ was recorded at ca. 300 K. These results imply different physical nature of phase transition in examined AILs. A valuable insight into this issue brings DSC experiments with various scanning rates.

As visible in Figure 1 SI, a slower heating rate moves the step-like increase of C_p towards lower temperatures for $[P_{666,14}][BOB]$, which indicates the kinetic nature of this phase transition and thus a simple vitrification process. On the other side of the spectrum is $[P_{666,14}][BF_4]$, where decreasing the scanning rate from 10 to 1 K/min shifted the crystallization onset from 227 K to 265 K, whereas the melting process occurred around 300 K in both cases. In turn, independently of the applied heating rate, phase 2 in four remaining AILs fully returned to phase 1, at the same temperature, with the only difference in ΔH, i.e., the lower the ramp rate, the higher the ΔH value. Notably, the phase 2 state is an optically transparent homogenous disordered phase, as confirmed by microscopic observations. These findings lead to conclusion that the liquid-liquid phase transition (LLT) occurs for $[P_{666,14}][TFSI]$, $[P_{666,14}][TCM]$, $[P_{666,14}][TAU]$ and $[P_{666,14}][SCN]$, in the latter case followed by cold crystallization and melting processes.

A closer inspection of the DSC results indicates that the temperature of LLT decreases in the following order: $[SCN]^- < [TAU]^- < [TCM]^- < [TFSI]^-$ that corresponds well with decreasing basicity and increasing anion size. Noteworthy, the large, rigid and non-coordinating $[BOB]^-$ drove vitrification rather than LL, although even larger but more flexible, lower symmetry $[TFSI]^-$ induced LL phase transition. Furthermore, the small, symmetrical and non-coordinating $[BF_4]^-$ induced crystallisation, whereas [SCN]-, which is small but has lower symmetry and higher basicity than $[BF_4]^-$, featured both LTT and crystallisation/melting behavior. It appears that LL phase transition is relatively easy to induce in $[P_{666,14}]$-based ILs, but certain conditions with respect to size, symmetry, conformational flexibility and possibly Lewis basicity of the anions must be met.

Changes in ion dynamics accompanying LLT. To further advance the knowledge on LLT in $[P_{666,14}]$-based ILs, dielectric spectroscopy has been employed. First, the single-frequency experiments, analogous to DSC scans, have been performed for selected AILs. The evolution of dielectric constant (ε') at 1MHz, accompanying cooling and subsequent heating of $[P_{666,14}][TFSI]$, $[P_{666,14}][TCM]$, $[P_{666,14}][BOB]$ and $[P_{666,14}][BF_4]$ at 1 K/min, is illustrated in Figure 2 SI. The $\varepsilon'(T)$ curves obtained for the $[TFSI]^-$ and $[TCM]^-$ samples reveal reversible character with a step-like signature of LLT. In turn, the behavior of ε' for $[P_{666,14}][BOB]$ and $[P_{666,14}][BF_4]$ resembles the characteristics of the liquid-glass transition and crystallization, respectively, which corresponds to calorimetric data.

To verify whether the LLT manifests itself in molecular dynamics behavior, the dielectric measurements over a wide frequency (10^{-2} – 10^7 Hz) and temperature range were performed. For ionic systems, the translational displacement of charge carriers (dc-conductivity) dominates the dielectric loss $\varepsilon''(f)$ function, conventionally employed for data analysis.[24] Therefore, complex electric conductivity $\sigma^*(f)=\varepsilon_0/Z^*(f)C_0$ and complex electric modulus $M^*(f)=1/\varepsilon^*$, are usually

adopted to express their dielectric properties.[25] The latter formalism allows for the determination of three relevant quantities describing the ion dynamics in AILs: dc-conductivity $\sigma_{dc}=2\pi f\varepsilon_0/M''$ calculated from a low-frequency region of M"; conductivity relaxation times $\tau_\sigma=1/2\pi f_{max}$ determined directly form M" maximum; and distribution of relaxation times reflected in the width of M"(f) peak. Therefore, this representation was selected to evaluate the data recorded in this work. $[P_{666,14}][BF_4]$ has been excluded from these studies due to the high tendency to crystallize. Figure 2A shows the representative electric modulus spectra of $[P_{666,14}]$[TFSI] collected at 0.1MPa and various temperatures. From this graph, it is apparent that the M"(f) peak shifts to lower frequencies upon cooling. This gradual change is in keeping with cooling effects seen in other ionic systems and reflects ions' suppressed mobility.[26] However, starting from a certain temperature, coinciding well with the calorimetric LLT, the temperature sensitivity of the σ-process becomes markedly stronger while the M" peak is broadening significantly. These effects, visualized for $[P_{666,14}]$[TFSI], are characteristic of all studied herein AILs except for $[P_{666,14}]$[BOB].

To quantify changes in the shape of conductivity relaxation peak across the LLT, the Kohlrausch function, function, $\phi(t) = exp[-(t/\tau_\alpha)^{\beta_{KWW}}]$,[27] has been used (an exemplary fitting curves are presented in Figure 2A). The β_{KWW} parameters obtained from fitting of M" peaks are plotted as a function of the frequency of M" peak maximum (f_{max}) (Figure 2B). It is well-known that the broader and more asymmetric the peak is, the lower is the value of β_{KWW}. The exponent characterizing the liquid 1 ($0.62<\beta_{KWW}<0.67$) falls in the middle of the range reported for various ionic glass-formers.[28] On the other hand, a transition to liquid 2 brings a substantial decrease of β_{KWW}. The most significant drop is denoted for AILs with $[TCM]^-$ and $[TFSI]^-$ anions, and the weakest occurs for the system with the $[TAU]^-$ anion. This observation indicates that the distribution of the relaxation times becomes broader during the transformation from liquid 1 to liquid 2. In other words, in liquid 1 the species are more dynamically correlated (i.e., components relax with similar τ_σ), whereas in phase 2 there is higher heterogeneity (i.e. some components are more mobile and some are less mobile). This result is in agreement with dielectric data measured across LLT for TTP.[29] In contrast, the shape of M"(f) function recorded for $[P_{666,14}]$[BOB] is invariant over the entire examined temperature range. Thus, the time-temperature superposition (TTS) rule, typical for glass-forming systems, is valid.

The temperature dependence of conductivity relaxation times $\tau_\sigma(T^{-1})$, calculated directly from the modulus peak maxima, also exhibits a peculiar behavior near the calorimetric LLT. In particular, τ_σ collected in liquid 1 reveals a typical non-Arrhenius behavior, and a substantial departure from the VFT law occurs at the onset of phase transition; that is, an abrupt increase is observed in apparent activation energy. A closer inspection of Figure 2C reveals similar values of $\tau_\sigma(T_{LL})$ for the studied AILs ($\log\tau_\sigma = -2.5\pm0.5$), far from the time scale commonly identified with the liquid-glass transition (τ_σ=100s). The LLT is also clearly detectable when the Stickel operator, $[d\log\tau_\sigma/d1000T^{-1}]^{-0.5}$, is applied; such procedure gives two linear regions that intersect at T_{LL} (Figure S3). Notably, the sign of LLT is also detectable in dc-conductivity behavior (see Figure S4).

The LLT under high-pressure conditions. Although rapid cooling is probably the most straightforward method for inducing a first-order phase transition, it is not the only route. The LLT of phosphorus[30] or nitrogen[31] can also be realized by isothermal compression. However, according

to experimental results reported in the literature, to induce LLT in these systems, extreme temperature and pressure conditions have to be applied, for example 50 GPa and 1920 K for nitrogen. In this context, one may question the possibility of achieving LLT in $[P_{666,14}]^+$ ILs through the isothermal compression.

Three ILs have been chosen for high-pressure tests: $[P_{666,14}][TCM]$ and $[P_{666,14}][TFSI]$ – as revealing the most spectacular changes in relaxation dynamics across the LLT at 0.1 MPa, as well as $[P_{666,14}][BOB]$ - as a counterexample. The representative high-pressure spectra collected at 223 K for $[P_{666,14}][TCM]$ are shown in Figure 3A. The observed pattern of behavior upon compression is analogous to the isobaric cooling experiment: despite maintaining the same pressure step, after reaching certain pressure the shifts in f_{max} are markedly faster. Also the shape of the M"(f) peak behaves similarly to the ambient pressure experiment - during the isothermal compression, past certain pressure the peaks broaden significantly. A direct comparison of the spectra collected at given f_{max} under various T-P conditions shows that the shape of the σ-relaxation is independent of thermodynamic variables if phase 1 is considered (Figure 3B). Such a phenomenon, called the temperature-pressure superposition principle, is a typical feature of glass-forming materials.[32] However, for superimposed spectra of liquid 2, the shape of M"(f) function at a given value of τ_σ becomes narrower with increasing T and P. In other words, compression at higher temperatures reduces the distribution of relaxation times in phase 2, making it more homogenous in terms of molecular dynamics. The same pattern has been detected for $[P_{666,14}][TFSI]$. In contrast, the σ-dispersion in $[P_{666,14}][BOB]$ has been constant at any chosen τ_σ (see Figure 3C). Consequently, the narrowing of M"(f) peak with pressure cannot be treated as a feature unique to $[P_{666,14}]^+$ ILs, but rather as a unique characteristic of the liquid-liquid transformation. This peculiar behavior is, to some extent, similar to the effect of pressure on polymerization reactions, when the material of a narrower distribution of molecular weight is obtained under higher pressure.[33]

The analysis of isothermal τ_σ-P dependences determined for the studied ILs reveals another intriguing feature of the liquid-liquid transition. As illustrated in Figures 4A-C, isothermal compression has fundamentally the same effect on the ion dynamics as isobaric cooling, i.e. the conductivity relaxation times τ_σ are getting longer with squeezing. The $\tau_\sigma(P)$ data of $[P_{666,14}][BOB]$ follow the pVFT behavior over the entire examined pressure range, while the experimental points recorded for $[P_{666,14}][TCM]$ and $[P_{666,14}][TFSI]$ markedly rise in slope at certain P bringing an almost four-fold increase in apparent activation volume $V^{\#}=2.303RT(d\log\tau_\sigma/dP)_T$. (Figures 4D and 4E). However, what is interesting, the kink of the τ_σ-P curve, being a manifestation of LLT, is independent of T-P conditions and appears at constant conductivity relaxation times for a given system; specifically, at τ_σ of 0.01 s for $[P_{666,14}][TFSI]$ and miliseconds for $[P_{666,14}][TCM]$. This result shows that in analogy to liquid-glass transition, the L-L transformation is isochronal in nature. Nevertheless, the time scale of ion dynamics at LLT, $\tau_\sigma(T_{LL},P_{LL})$ is not universal but depends on intermolecular interactions.

Defining P_{LL} as the pressure at which the activation volume starts to increase, we obtain the pressure dependence of T_{LL} plotted in the inset in Figure 4. As presented, T_{LL} increases with pressure in a linear fashion, with the slope equal to 81 K/GPa for $[P_{666,14}][TFSI]$ and 87 K/GPa for $[P_{666,14}][TCM]$. It means that the pressure in the order of 1.2 GPa is required to observe the L-L phenomenon at room temperature conditions. Interestingly, when the isothermal $\tau_\sigma(P)$ data are crossed at τ_σ=100s, non-linear $T_g(P)$ dependences with the dT_g/dP coefficient of 125±5 K/GPa is

obtained for $[P_{666,14}][TFSI]$, $[P_{666,14}][TCM]$ and $[P_{666,14}][BOB]$. This indicates that dynamics of phase 2 of $[P_{666,14}][TFSI]$ and $[P_{666,14}][TFSI]$ freezes (transform to glass) with the same characteristic as supercooled liquid of $[P_{666,14}][BOB]$.

The determined values of dT_{LL}/dP offer a unique possibility to estimate the variations in volume accompanying the LLT (ΔV_{LLT}) using a simple Clausius-Clapeyron equation, $dP/dT=\Delta S_{LLT}/\Delta V_{LLT}$. The ΔS_{LLT} denotes the entropy changes during the LLT and can be obtained as $\Delta S_{LLT} = \Delta H_{LLT}/T_{LLT}$, where ΔH_{LLT} is the enthalpy of first-order transition. The calculated values of ΔV_{LLT} are equal to 0.00583 $cm^3\ g^{-1}$ and 0.00387 $cm^3\ g^{-1}$ for $[P_{666,14}][TCM]$ and $[P_{666,14}][TFSI]$, respectively. To put these numbers into perspective, we measured the density changes of these ILs as a function of temperature and extrapolated the obtained dependence to T_{LLT} (see Figure S5). Such procedure gives V_{LLT} = 0.87591 $cm^3\ g^{-1}$ for $[P_{666,14}][TFSI]$ and 1.04515 $cm^3\ g^{-1}$ for $[P_{666,14}][TCM]$, indicating that changes of around 0.5% occur at LLT, that is within the error in dilatometric measurements. These small variations in the specific volume can be easily overlooked in direct measurements of V(T,P) and reveal that density is not the dominant order parameter governing the LLT in ILs. This is in agreement with the experimental data recorded for sodium acetate trihydrate ($CH_3COONa\cdot 3H_2O$) where a first-order LLT without density discontinuity was identified.[17] Moreover, LLTs without density change were suggested to take place in several metallic glass-formers.[34]

In summary, our findings provide experimental support for the hypothesis that the LLT occurs in ion-containing systems. Our studies of a series of $[P_{666,14}]^+$-based AILs and six different anions demonstrate that the LLT occurs in AILs with $[TCM]^-$, $[TFSI]^-$, $[TAU]^-$ and $[SCN]^-$ anions, but not with $[BOB]^-$ (showing vitrification) and $[BF_4]^-$ (showing crystallization). This demonstrates that ILs can be fine-tuned to display T_{LL}, which is dependent on several parameters, such as anion size, geometry, conformational flexibility, Lewis basicity and the strength of interionic interactions. Our study also provides an important approach to the LLT-correlated properties. We found that the parameters characterizing the ion dynamics (τ_σ, σ_{dc}) and distribution of relaxation times (β_{KWW}) monitored on isobaric cooling and isothermal compression reveal non-monotonic behavior identified with LLT. Furthermore, independently of T-P conditions, the sign of LLT is observed at τ_σ=*const.* within a given system, i.e., it occurs at a certain time scale of ionic motions dependent on interionic interactions. Upon transition liquid 1→liquid 2 (induced by cooling or high-pressure), the AILs become more heterogenous in terms of ion mobility. Additionally, the dT_{LL}/dP coefficient determined for [TCM] and [TFSI]-based ILs in high-pressure experiment, together with ΔH_{LL} and T_{LL} let us estimate the volume changes accompanying LLT by using the Clausius-Clapeyron equation. We found that ΔV_{LL} is very small and can be undetectable in conventional dilatometry measurement. Such an LLT may offer a unique opportunity for investigating the subtle structural and dynamic changes of liquid, which could be a critical step for understanding liquids.

Methods

Differential Scanning Calorimetry (DSC). Calorimetric experiments of studied ILs were performed by means of a Mettler Toledo DSC1STAR System equipped with a liquid nitrogen cooling accessory and an HSS8 ceramic sensor (a heat flux sensor with 120 thermocouples). Each sample with a mass of around 10-

20 mg was measured in aluminum crucibles with a 40 μL volume. Prior to the measurement, the samples were annealed 30 min at 373 K. Temperature ramps involved cooling to 143 K and then heating to 373 K with a rate of 10 K/min. Samples were cycled at least 3 times to ensure reproducibility and high accuracy. During the experiments, the flow of nitrogen was kept at 60 mL min^{-1}. Enthalpy and temperature calibrations were performed using indium and zinc standards.

Dielectric Measurements. The dielectric measurements at ambient pressure for studied ILs were carried out over a frequency range from 10^{-1} Hz to 10^{7} Hz by means of Novo-Control GMBH Alpha dielectric spectrometer. The temperature was controlled by the Novocool system with the accuracy of 0.1 K. During this measurement, the sample was placed between two stainless steel electrodes (diameter = 15 mm). The distance of 0.08 mm was provided by the quartz ring. For the pressure dependent dielectric measurements, we used the capacitor, filled with the studied sample, which was next placed in the high-pressure chamber and compressed using the silicone oil. Note that during the measurement the sample was only in contact with stainless steel. The pressure was measured by the Unipress setup with a resolution of 1 MPa. The temperature was controlled within 0.1 K by means of a Weiss fridge.

Table 1 The thermodynamic characterization of studied systems. T_{LL} and ΔH denote respectively the temperature and enthalpy of liquid-liquid transition determined during the cooling (c) and heating (h) scan. T_g-glass transition temperature, T_c-crystallization temperature, T_m-melting temperature, ΔH_m – enthalpy of melting, ΔH_c – enthalpy of crystallization, v-molecular volume of anions.

	T^{c}_{LLT}	T^{h}_{LLT}	$-\Delta H^{c}_{LLT}$	ΔH^{h}_{LLT}	T_g	T_c	T_m	ΔH_m	ΔH_c	v	*Donor Numbers*
	K	K	J g^{-1}	J g^{-1}	K	K	K	J g^{-1}	J g^{-1}	nm^3	kcal mol^{-1}
$[SCN]^-$	208.2	212.5	15.0	17.2	-	263.0	275.0	18.7	17.7	0.071	45.9
$[BF_4]^-$	-	-	-	-	-	265.0* 227.3	300* 298.9	61.38* 61.65	49.26* 21.83	0.079	7.3
$[TAU]^-$	209.4	210.2	4.3	5.8	-	-	-	-	-		
$[TCM]^-$	204.4* 203.2*** 202.2	206.9* 207.5** * 206.6	13.7* 10.1*** 8.2	13.7* 9.8*** 8.9	-	-	-	-	--	0.121	26.1
$[BOB]^-$	-	-	-	-	202.7	-	-	-	-	0.174	
$[TFSI]^-$	200.5* 200.1** 199.6*** 199.4	203.1* 203.3** 203.8** * 204.0	8.6* 7.3** 6.5*** 5.9	9.7* 8.2** 7.1*** 6.6	-					0.230	11.2

* 1 K/min; ** 2 K/min;*** 5 K/min; Others: 10 K/min

Molecular volume of ions was taken from refs. [35,36]

An increase of ΔH_{LL} with decrease of scanning rate indicates that phase 1 needs a certain amount of time for transfer to phase 2.

Figures

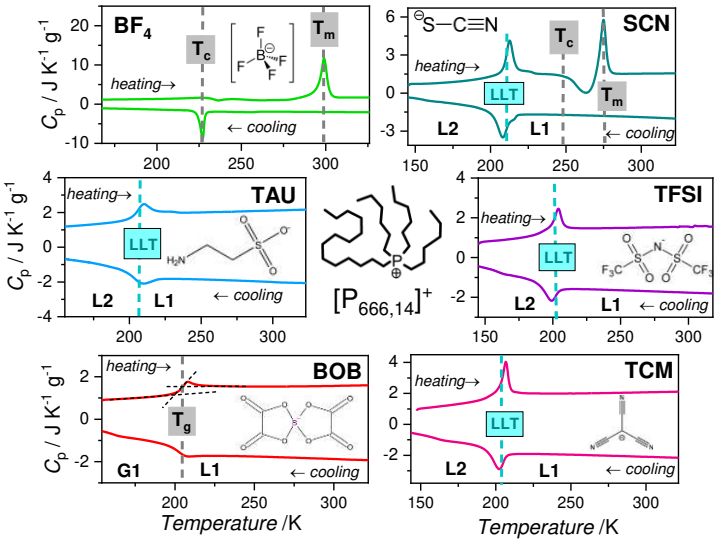

Figure 1 DCS traces of $[P_{666,14}]^+$-based ILs. The data were collected on cooling and subsequent heating with the rate of 10K/min. (Endo up). The ΔH values determined for the symmetrical peaks on heating and cooling are in good agreement with each other for four AILs: $[TFSI]^-$, $[TCM]^-$, $[TAU]^-$, $[BOB]^-$ and $[SCN]^-$. This contrasts with $[P_{666,14}][BF_4]$, for which the enthalpy of the endothermic peak is five times larger than those of other AILs studied here, and differs significantly from the enthalpy of the exothermic feature (Table 1).

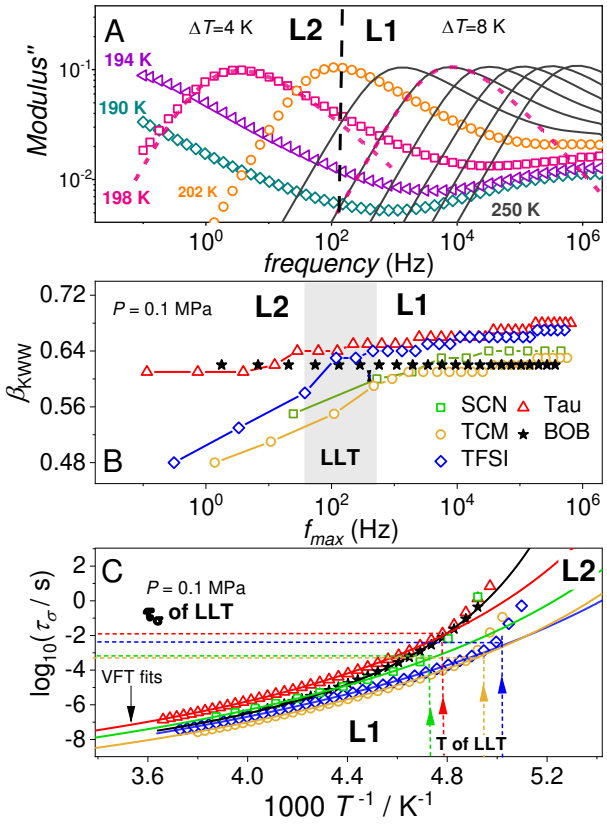

Figure 2 Dielectric response of studied ILs measured at ambient pressure conditions. A) The representative dielectric data of $[P_{666,14}][TFSI]$ in liquid 1 (solid lines) and liquid 2 (scatters) phases recorded on cooling and presented in electric modulus representation. Dashed lines denote fits of KWW function to experimental data with β_{KWW}=0.65 and 0.53, in liquid 1 and liquid 2, respectively. B) The β_{KWW} exponent plotted as a function of the frequency of modulus peak maximum. C) Temperature dependence of conductivity relaxation time for all studied herein ILs. Solid lines denote the fit of VFT function $\tau_\sigma = \tau_\infty exp(\frac{DT_0}{T-T_0})$ to experimental data. Dashed lines indicate T_{LL} and τ_σ at LLT.

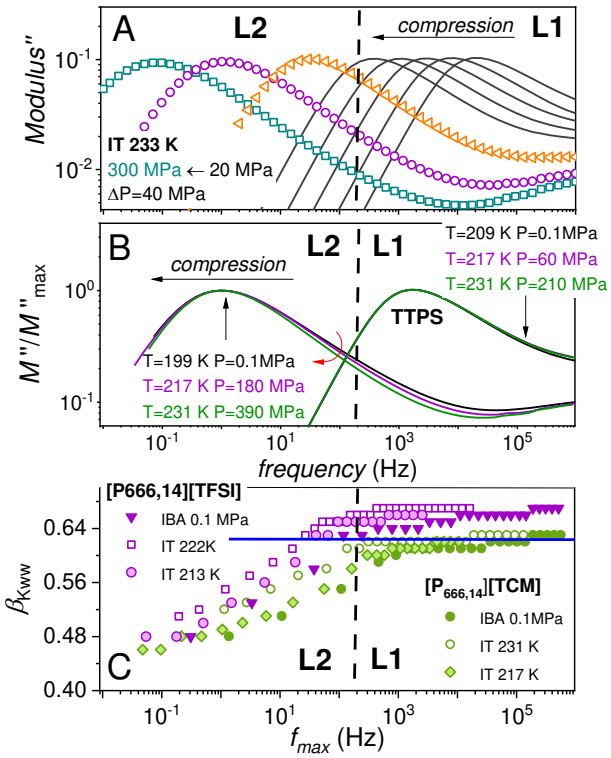

Figure 3 Dielectric response of studied ILs measured at high-pressure conditions. A) The representative dielectric data recorded for $[P_{666,14}][TCM]$ in liquid 1 (solid lines) and liquid 2 (scatters) phases, recorded during compression and presented in electric modulus representation. B) The representative M"(f) spectra of $[P_{666,14}][TCM]$ recorded at various T-P conditions; however the same τ_σ superimposed to each other in liquid 1 and liquid 2, respectively. C) The β_{KWW} exponent plotted as a function of the frequency of modulus peak maximum at various thermodynamic conditions. IBA denotes 0.1 MPa and various temperatures while IT denotes isotherm and various pressure. The horizontal line indicates β_{KWW} for $[P_{666,14}][TCM]$ being constant at various T-P conditions.

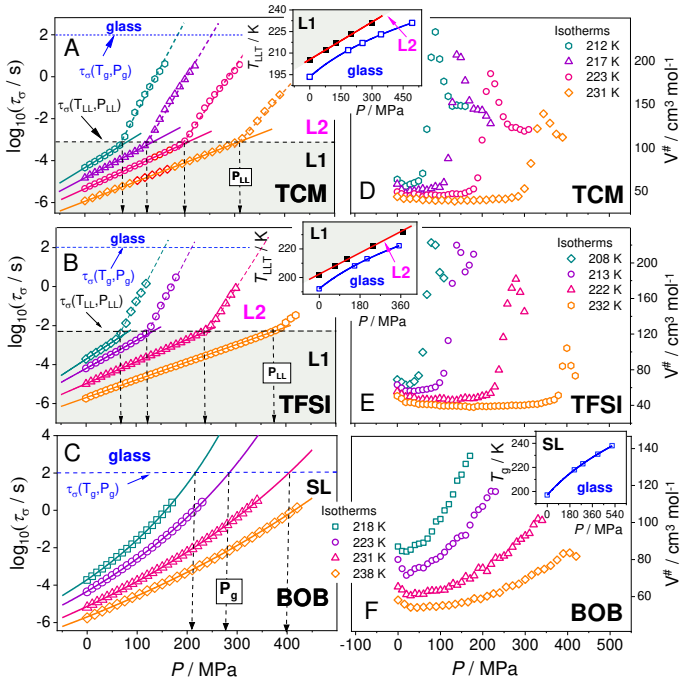

Figure 4 High-pressure data of selected ILs. Panels A B and C present the pressure dependence of conductivity relaxation time measured at various T. Solid lines denote the pVFT fit $\tau_\sigma = \tau_0 exp(\frac{BP}{P_0 - P})$ to experimental data. Dashed lines indicate P_{LL} and τ_σ at LLT. Panels D, E, F present pressure dependence of apparent activation volume, $V^{\#}$. The four-time increase in $V^{\#}$ at LLT indicates a formation of non-polar domains of large scale in liquid 2. Considering the very bulky cation and much smaller anions, it could be speculated that cations becomes partially "locked" into positions, whereas anions are free to move in channels of non-polar domains.
In the inset T_{LL} and T_g as a function of P is presented.

Acknowledgments

Authors acknowledge M. Musiał for the density measurements of [$P_{666,14}$][TCM]. The authors are deeply grateful for the financial support by the National Science Centre within the framework of the Opus15 project (grant nr DEC- 2018/29/B/ST3/00889). Solvay is acknowledged for kindly providing trihexyl(tetradecyl)phosphonium chloride.

Author contributions

Z.W. conceived the project; S.C. planned and carried out the experimental work; S.C. analyzed the data; Z.W. prepared the figures; S.L. and Y.D. synthesized and characterized the ionic liquids,

under the supervision of M. S.-K.; Z.W. wrote the paper with input and advice from M.S-K. and M.P.; M.P. supervised the project.

Competing interests. The authors declare no competing financial interests

Supplementary information contains synthesis protocol of ILs, results of DSC and BDS experiments.

References

[1] Angell, C. A. Formation of glasses from liquids and biopolymers. *Science* **267**, 1924–1935 (1995).
[2] Adam, G. & Gibbs, J. H. On the temperature dependence of cooperative relaxation properties in glass-forming liquids. *J. Chem. Phys*. **43**, 139–146 (1965).
[3] Katayama, Y.; Mizutani, T.; Utsumi, W.; et al. A first-order liquid−liquid phase transition in phosphorus. *Nature* **403**, 170−173 (2000)
[4] Sastry, S.; Angell, C. A. Liquid−liquid phase transition in supercooled silicon. *Nat. Mater*. **2**, 739−743, (2003)
[5] Saika-Voivod, I., Poole, P. H. & Sciortino, F. Fragile-to-strong transition and polyamorphism in the energy landscape of liquid silica. *Nature* **412**, 514–517 (2001).
[6] Glosli, J. N.; Ree, F. H. Liquid-liquid phase transformation in carbon. *Phys. Rev. Lett*. **82**, 4659, (1999)
[7] Sheng, H. W. et al. Polyamorphism in a metallic glass. *Nat. Mater*. **6**, 192–197 (2007).
[8] Xu, W.; Sandor, M. T.; Yu, Y.; et al. Evidence of liquid−liquid transition in glass-forming La50Al35Ni15 melt above liquidus temperature. *Nat. Commun*. **6**, 7696 (2015)
[9] Greaves, G. N. et al. Detection of first-order liquid/liquid phase transitions in yttrium oxide-aluminum oxide melts. *Science* **322**, 566–570 (2008).
[10] Wei, S. et al. Liquid–liquid transition in a strong bulk metallic glass-forming liquid. *Nat. Commun*. **4**, 2083 doi: 10.1038/ncomms3083 (2013).
[11] Angell, C. A. Insights into phases of liquid water from study of its unusual glass-forming properties. *Science* **319**, 582–587 (2008).
[12] Ito, K., Moynihan, C. T. & Angell, C. A. Thermodynamic determination of fragility in liquids and a fragile-to-strong liquid transition in water. *Nature* **398**, 492–495 (1999).
[13] Kurita, R. & Tanaka, H. Critical-like phenomena associated with liquid-liquid transition in a molecular liquid. *Science* **306**, 845–848 (2004).
[14] Tanaka, H.; Kurita, R.; Mataki, H. Liquid-liquid transition in the molecular liquid triphenyl phosphite. *Phys. Rev. Lett.* **92**, 025701 (2004)
[15] Kobayashi, M. Tanaka, H. The reversibility and first-order nature of liquid-liquid transition in a molecular liquid. *Nat. Commun*. **7**, 1–8 (2016).
[16] Tanaka , H . General view of a liquid-liquid phase transition . Phys. Rev. E 62 , 6968 – 6976 (2000).
[17] Liu, X., Liu, S., Chen, E., Peng, L., Yu, Y. First-Order Liquid−Liquid Transition without Density Discontinuity in Molten Sodium Acetate Trihydrate and Its Influence on Crystallization, *J. Phys. Chem. Lett*. **10**, 4285−4290 (2019)
[18] Zeng, Q. et al. Origin of pressure-induced polyamorphism in Ce75Al25 metallic glass. *Phys. Rev. Lett*. **104**, 105702 (2010).
[19] Liu, L., Chen, S.-H., Faraone, A., Yen, C.-W. & Mou, C.-Y. Pressure dependence of fragile-to-strong transition and a possible second critical point in supercooled confined water. *Phys. Rev. Lett*. **95**, 117802 (2005).
[20] Armand, M., Endres, F., MacFarlane, D. R., Ohno, H. and Scrosati, B. Ionic-liquid materials for the electrochemical challenges of the future *Nat. Mater*. **8** 621–9 (2009)

[21] Angell, C.A., Xu, W., Yoshizawa, M., Hayashi, A., Belieres, J-P., Lucas, P. and Videa, M. 2005 Physical chemistry of ionic liquids, inorganic and organic, protic and aprotic Chemistry of Ionic Liquids ed H Ohno (New York: Wiley) pp 5–23

[22] Harris, M.A., Kinsey, T., Wagle, D.V., Baker, G.A. & Sangoro, A. Evidence of a liquid–liquid transition in a glass-forming ionic liquid, *PNAS*, **118**, 11 (2021)

[23] Fraser, K. J., MacFarlane, D.R. Phosphonium-based ionic liquids: An overview. *Aust. J. Chem*. **62**, 309–321 (2009).

[24] Kremer, F., Schonhals, A. Eds., Broadband Dielectric Spectroscopy (Springer, New York, NY, 2003).

[25] Sangoro J. R., Kremer F., Charge transport and glassy dynamics in ionic liquids. *Acc. Chem. Res*. **45**, 525–532 (2012).

[26] Paluch, M. Dielectric properties of ionic liquids; Springer: Berlin, 2016.

[27] Ngai, K. L., Greaves, G. N. and Moynihan, C. T. Correlation between the activation energies for ionic conductivity for short and long time scales and the Kohlrausch stretching parameter β for ionically conducting solids and melts *Phys. Rev. Lett*. **80** 1018 (1998)

[28] Wojnarowska, Z.; Paluch, M. Recent progress on dielectric properties of protic ionic liquids. *J. Phys.: Condens. Matter* **2015**, 27, 913 073202.

[29] R. Kurita, H. Tanaka, Control of the fragility of a glass-forming liquid using the liquid lquid phase transition. *Phys. Rev. Lett*. **95**, 1–4 (2005).

[30] Monaco, G., Falconi, S., Crichton, W. A. & Mezouar, M . Nature of the first order phase transition in fluid phosphorus at high temperature and pressure . *Phys. Rev. Lett*. **90** , 255701 (2003).

[31] Mukherjee, G.D. & Boehler, R. High-Pressure Melting Curve of Nitrogen and the Liquid-Liquid Phase Transition. *Phys. Rev. Lett.* **99**, 225701 (2007)

[32] Floudas G, Paluch M, Grzybowski A and Ngai K L 2011 Molecular Dynamics of Glass-Forming Systems: Effects of Pressure 1st edn (Berlin: Springer)

[33] Dzienia, A., Maksym, P., Tarnacka, M., Grudzka-Flak, I., Golba, S., Zięba, A., Kaminski, K., Paluch, M. High pressure water-initiated ring opening polymerization for the synthesis of well-defined α-hydroxy-ω-(carboxylic acid) polycaprolactones, *Green Chemistry*, **19**, 15, 3618-3627 (2017)

[34] Aasland, S. & McMillan, P. F. Density-driven liquid-liquid phase separation in the system Al2O3-Y2O3. *Nature* **369**, 633–636 (1994).

[35] Marcus, Y. Ionic and molar volumes of room temperature ionic liquids. *J. Mol. Liq.* **2015**, *209*, 289-293

[36] Beichel, W.; Preiss, U. P.; Verevkin, S. P.; Koslowsli, T.; Krossing, I. Empirical description and prediction of ionic liquids' properties with augmented volume-based thermodynamics. *J. Mol. Liq.* **2014**, *192*, 3-8

Supplementary Files

This is a list of supplementary files associated with this preprint. Click to download.

- P66614SI.docx